Acta Biologica Hungarica 68(3), pp. 267–278 (2017)
DOI: 10.1556/018.68.2017.3.4

FUSIFORM VATERITIC INCLUSIONS OBSERVED IN EUROPEAN EEL (*ANGUILLA ANGUILLA* L.) SAGITTAE

Zoltán Kern,[1]* Miklós Kázmér,[2] Tamás Müller,[3] András Specziár,[4] Alexandra Németh[1] and Tamás Váczi[5]

[1]Institute for Geological and Geochemical Research, MTA Research Centre for Astronomy and Earth Sciences, Budaörsi út 45, H-1112 Budapest, Hungary
[2]Department of Palaeontology, Eötvös University, Pázmány Péter sétány 1/c, H-1117 Budapest, Hungary
[3]Department of Aquaculture, Faculty of Agricultural and Environmental Sciences, Szent István University, H-2100 Gödöllő, Hungary
[4]Balaton Limnological Institute, MTA Centre for Ecological Research, H-8237 Tihany, Hungary
[5]Department of Mineralogy, Eötvös Loránd University, Pázmány Péter sétány, 1/c, H-1117 Budapest, Hungary

(Received: January 12, 2017; accepted: March 27, 2017)

Microscopic inclusions have been observed in 7 out of 106 European eel (*Anguilla anguilla* L.) sagittae using polarizing microscope and scanning electron microscope meanwhile the annual increments were studied to characterize the age structure of the population living in Lake Balaton. The presence of vaterite, a rare calcium carbonate polymorph was observed in these inclusions using Raman spectroscopy. Vateritic sagittae in wild fish are usually considered as symptom of physiological stress. The observed fusiform inclusions represent a new morphological type of vaterite inclusions in eel otolith. Two alternatives are hypothesized to explain their formation: 1) metabolic disorder, such as erroneous protein synthesis; 2) introduction of an alien protein into the eel's inner ear. The origin and physiological significance of this new morphological type of vateritic inclusions is still an open question. Same as whether it can be found in other species or specific only to eel otoliths.

Keywords: Anguilla – otolith – sagitta – vaterite – aragonite

INTRODUCTION

The inner ear of teleost fishes includes three semicircular canals and three otolithic organs (sacculus, utricle and lagena). Each contains three pairs of small carbonate structures (sagitta, asteriscus and lapillus, respectively), the so-called otoliths [28]. The largest of these, and consequently the most frequently studied, is the sagittal otolith, which is located in the sacculus of the membranous labyrinth. The dominant substrate of these biomineralized products is $CaCO_3$ which is deposited onto a few percent of organic matrix, including proteins (e.g., otolin-1, OMP-1, otoconin 90) and collagen [5, 34, 45]. This organic matrix is thought to play a definite role in the process of biomineralization. Recent studies of biominerals (particularly carbonates)

*Corresponding author; e-mail address: Kern.Zoltan@csfk.mta.hu

showed that an amorphous gel phase is deposited first, which is later crystallised to form a particular polymorph in the desired crystallographic orientation. This process is supposedly coordinated by the organic matrix included within the gel [3, 8, 9].

The dominant mineralogical phase constituting teleost sagittae is aragonite. The occurrence of different $CaCO_3$ polymorphs in teleost otoliths, however, is well documented [15]. Most notable is vaterite, a rare $CaCO_3$ polymorph. In contrast to orthorhombic aragonite the crystal structure of the vaterite polymorph still remains puzzling [6, 25].

A recent study found very high acid soluble protein content in vaterite pearls compared to the aragonitic ones [30] that together with earlier results [12, 49], suggest that acidic amino acid rich proteins play an important role in the polymorph selection during calcium carbonate biomineralization supposedly due to more abundant Ca^{2+} ion bonding sites provided by the carboxyl group of aspartic and glutamic acids.

Earlier observations described characteristic external features of vateritic otoliths as spherical or finger-like aggregates (so-called botryoidal surface) with glassy appearance [4, 15, 16, 29, 33, 38, 47]. These make them easily distinguishable from normal sagittae. Vateritic otoliths were identified in anguillid eels as well and polymorphic replacement appeared as vateritic sectors and mosaics in polished otolith transects [23, 24, 50].

Vateritic sagittae are usually considered as a stress symptom. Physiological stress associated with elevated water temperature [14], increased population density [42] or a habitat transition [29] have been addressed as potential factors in abnormal otolith development.

We present a new morphological type of vateritic inclusion in this brief report. This new type of vateritic inclusion was observed while studying microtexture of sagittal otoliths from European eels captured from Lake Balaton in Hungary.

MATERIAL AND METHODS

Sample collection and preparation

The microstructure of sagittal otolith of European eels (*Anguilla anguilla*) ($n = 8$) from the 2010 electrofishery in Lake Balaton, were studied. Eels were anaesthetised by using clove oil (*Syzygium aromaticum* (L.)) in the water (10 drop/10 L) and then euthanized by decapitation and their otoliths were removed. Following the realization of the unusual morphological type of inclusions, further samples ($n = 98$), captured in 2002 and 2003, still available from an earlier study [11] were also scrutinized.

Three samples were selected to illustrate the presentation of our results. Table 1 provides the basic information about the specimens.

Sagittae were embedded in epoxy resin. Embedded samples were ground until primordia were visible. Petrographic thin sections (~30 μm thickness) or "thick" sections grinding only one side of the embedded sagitta were prepared. A sequence of water based diamond suspensions (9, 6, 3, 1 μm; METADI®) was used for grinding

Table 1
Biological information on three selected European eels (*Anguilla anguilla*) used for otolith microtexture examination by scanning electron microscope and/or phase identification by Raman spectroscopy

Date of capture	Weight (g)	Length (mm)
17.06.2010	948	760
30.05.2003	305	568
30.05.2003	339	590

and alumina (0.05 μm, Gamma Micropolish® II) was used for polishing. Prior to analysis, samples were placed in distilled water and cleaned for 15 minutes using a (Badelin Sonorex DT-100) ultrasonic cleaner.

Analytical methods

Polished surface of thick sections were analysed by scanning electron microscopy (SEM) using a FEI Quanta 3D FIB/SEM instrument (beam: 15 kV, working distance: 10 mm). For detailed descriptions of the instrument see [18, 22]. Micromorphological and optical properties were investigated using a petrographic microscope (Nikon Eclipse E600 Pol and attached Spot insight camera), under both normal and polarized illumination to observe microstructural and crystallographic differences between inclusions and host material.

Raman microspectroscopy is a routinely used technique to study small-scale mineralogical properties, also in fish otoliths [17, 48, 50]. Raman spectroscopic analysis was conducted using a HORIBA JobinYvon LabRAM HR dispersive, edge-filter based confocal Raman spectrometer (focal length: 800 mm) equipped with an Olympus BXFM microscope and a thermoelectrically cooled CCD detector. Spectra were taken using the 785 nm emission of a diode laser, a 100× (N.A. 0.9) objective, a grating with 600 grooves/mm and a confocal pinhole of 100 μm, which acted also as the entrance slit to the spectrometer. The Rayleigh line was used for the spectral calibration of the spectrograph. Net counting times were between 30 and 60 s. Analysis spots were selected in such a way that the analyzed inclusions were not exposed to the polished surface. Contamination due to sample preparation or analysis therefore can safely be ruled out.

RESULTS

Scanning electron microscope (SEM) analysis revealed porous inclusions as compared to the host matrix in some sagittae. A distinct core region could be observed at most of them. Random sections cut through the inclusions and exposed in the polished surface clearly indicate that the objects have a spindle-like shape that is wider and circular in the middle and tapers at both ends when seen in cross-section (Fig. 1).

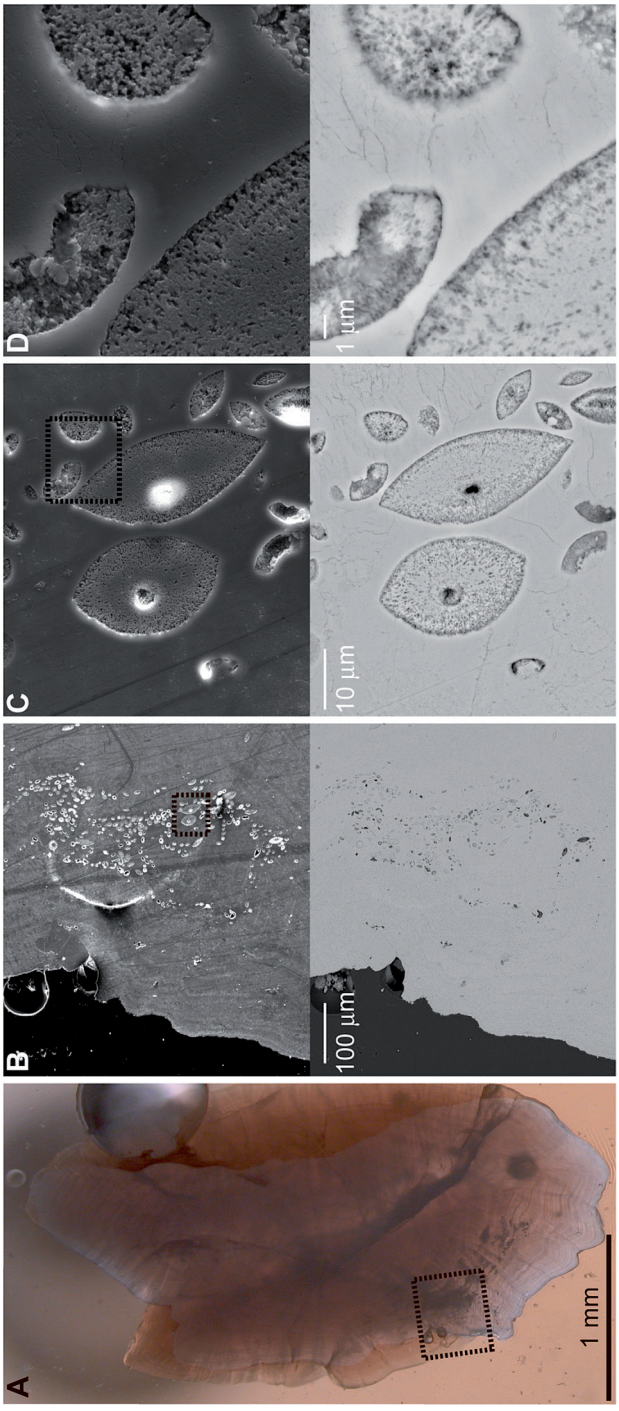

Fig. 1. Microscopic view of a polished eel sagitta with abundant inclusions. (MTl in Tab. 1) A: Inclusion-rich zones appear as dark clouds within the transparent host matrix as viewed in transmitted light. B–D: Magnification series of scanning electron micrographs showing the (micro)texture of the new morphological type of inclusions. Secondary and backscattered electron images are shown in the top and bottom, respectively. Dashed squares indicate the magnified area

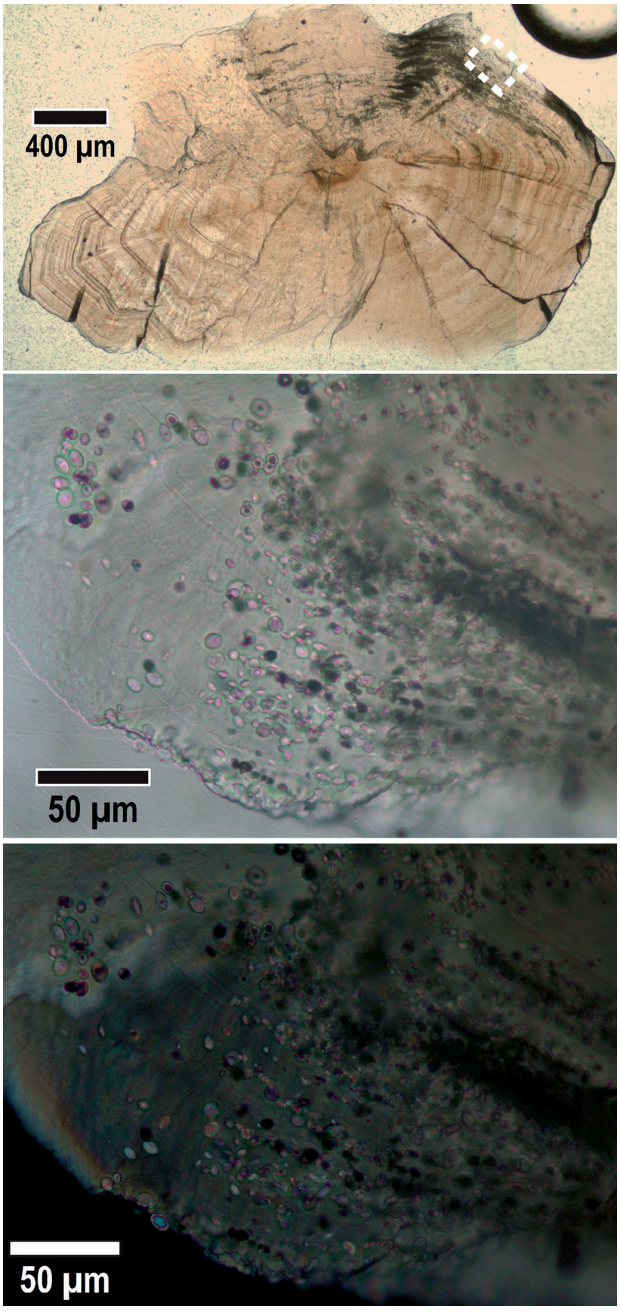

Fig. 2. Micrographs show the optical properties of the fusiform inclusions observed in eel (MT15 in Tab. 1) sagitta and their host material. Top: Full view under transmitted light. Dashed rectangle show the field enlarged below. Middle: Zoomed to the inclusion rich marginal field (single nicols), Bottom: Same view with crossed nicols

Largest observed axis was ~30 μm and the largest section perpendicular to this axis is <20 μm in diameter. These fusiform inclusions have been observed in 7 out of the studied 106 sagittae.

Observed basic optical properties are the following:

– the extinction of these inclusions under crossed polarisers is uniform and they usually show extinction in a phase opposite to the otolith background;
– they are highly birefringent: the interference colour varies between third order blue (in the centre of the inclusions) and magenta (near the rim) (Fig. 2). Considering

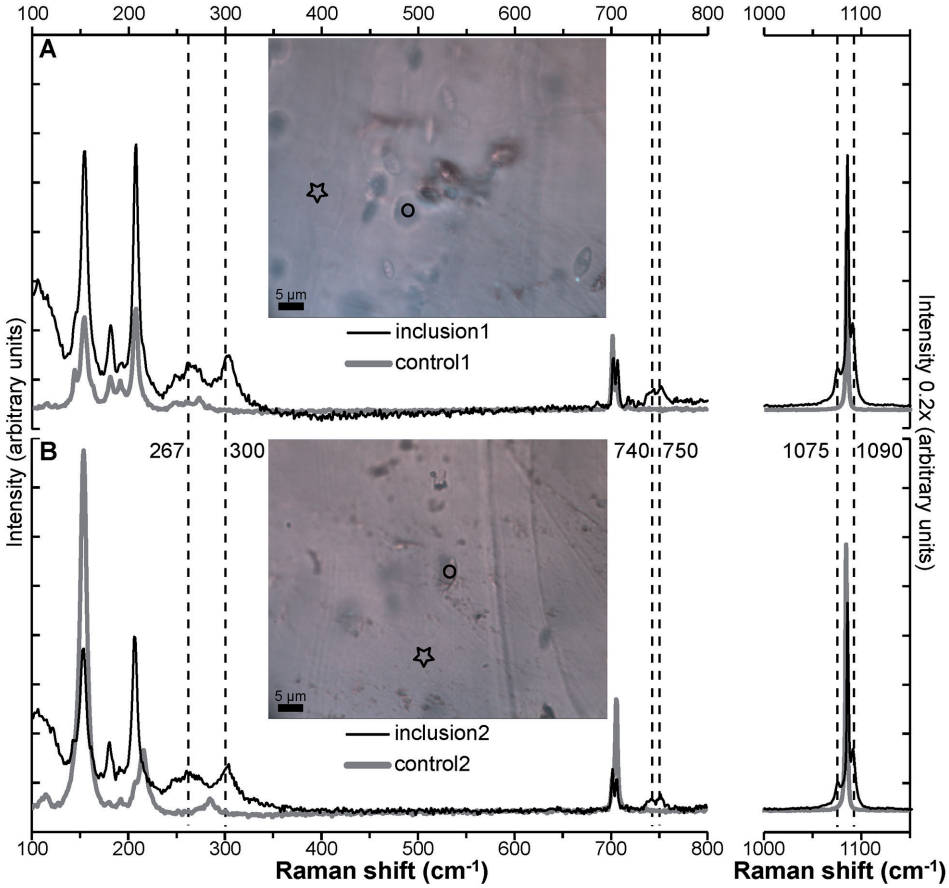

Fig. 3. Raman spectra obtained from inclusions and host aragonite. Analyses performed on inclusions and adjacent, inclusion-free control spots at two selected sectors of an eel otolith (MT18 in Tab. 1) (A, B). Investigated sectors with numerous fusiform inclusions viewed in transmitted light are shown as inset image above the corresponding Raman spectra. For better visualization, the spectra beyond 1000 cm^{-1} are scaled to 0.2× in intensity. Analysed spots are marked with circle (inclusion) and star (host aragonite) in the images. Characteristic Raman bands for vaterite, marked by dashed vertical lines, and corresponding wavenumbers are indicated. The vaterite signal was only observed from the inclusions. Note that the Raman spectra from inclusions show bands of both vaterite and aragonite because the confocal settings and inclusion dimensions did not allow a complete elimination of the host aragonite signal

that the thickness of vertical sections of these inclusions varies between 5–10 μm due to their small size a fourth-order interference colour was expected for a 30 μm thick section.

We established using the Becke line method that, regarding their current orientation, the refractive index of the inclusions was smaller than that of the surrounding aragonite.

As expected, the Raman spectra of the host material correspond to the aragonite phase [51], however, spectra obtained from the fusiform inclusions showed additional bands (Fig. 3). These bands did not match those of aragonite, and unambiguously identified vaterite [13, 31] in the fusiform inclusions (Fig. 3). It is to be noted that the confocal selectivity of the Raman instrument with the applied settings and the small size of the inclusions prevented acquiring pure vaterite spectra, but the spectral subtraction of the host spectra yielded pure vaterite spectra for identification.

DISCUSSION

Vateritic inclusions have already been identified in eel otoliths [23, 24, 50]. However, the observed fusiform inclusions represent a new morphological type of vaterite inclusions in eel otolith compared to the earlier reported vaterite mosaics.

Bands of inclusions nicely fit to the increment zones and incompletely enclosed (semi)inclusions have been observed at the otolith edge in some specimens (Fig. 2). This situation clearly indicates that the fusiform objects had been formed separately and attached later to the aggrading otolith surface. This suggests the co-existence of the fusiform objects as vateritic otoconia in the sacculus near the aragonitic sagitta.

The co-occurrence of vateritic otoconia and aragonitic sagitta in the sacculus have been already reported for a few fishes [16], although not for anguillid species.

Traditionally two driving forces may be identified within the endolymph to promote carbonate deposition: the ionic and organic states of the endolymph [36]. However, fish endolymph is usually considered as a highly supersaturated fluid [44] so it is unlikely to pose any obstacle in crystallization.

Since biomineralized aragonite and vaterite are characterized by a distinct protein matrix [12, 30] two possibilities can be explored: 1) the non-normal protein was produced by the eel, 2) if the eel's endolymphatic organ was properly functioning, what is the origin of the vaterite-related protein and, in general, the fusiform vateritic aggregates.

Normally, the proteins of the endolymph, making-up the protein matrix as well, are secreted by ionocytes, which are a small class of saccular epithelial cells [37]. Based on *in vitro* experiments employing recombinant otoconial matrix proteins it was shown that an incompletely folding variant of protein matrix of aragonitic otoconia resulted in vaterite biomineralization [46]. Deprivation of certain amino acids might cause misincorporation of another amino acid and results recombinant protein [35]. This type of protein coding error has already been addressed earlier to interpret the co-existence of polymorphs in otoliths [15].

It is also possible that the formation of the vaterite inducing protein and presence of the fusiform inclusions in the sagittae is a genetically determined trait, typical only for a smaller fraction the eel population. The relatively low occurrence rate might support this explanation. A comparative genetic analysis could provide direct evidence in this respect.

For the alternative scenario (i.e. the vaterit-forcing protein was not secreted by the epithelia cells) first we need to understand the vaterite mineralization in the aragonite producing environment. Most fishes with aragonitic sagittae have asterisci entirely made of vaterite [7, 26, 32], indicating that different polymorphs can be precipitated simultaneously, despite the shared endolymph [15]. This indicates that highly localized saturation conditions may exist within the endolymph allowing a change in biomineralization within a very small distance [47].

In addition, we note that the porous structure, the vateritic mineralogy and the distinct core of these inclusions resemble to the characteristics described from bacterially mediated biomineralized spherulites [19, 39]. Based on these observations it is assumed that bacterial (or viral) production might introduce an alien protein into the eel's endolymph.

Assuming that the fusiform vateritic objects are linked to bacterial (or viral) activity the relatively low occurrence rate (6–7%) does not necessarily reflect the proportion of infected specimens in the population. For instance, the effect could escalate to such a degree which can cause disturbed biomineralization in the endolymph only in the specimens with weakened health status. As noted above explanatory ecological and environmental factors frequently accounted for the usual mosaic vaterite replacement in otoliths are elevated water temperature [14], increased population density [42], and habitat transition [29]. Elevated water temperature, increased population density can be ruled out in the case of Balaton. The average water temperature was relatively constant (between 10 and 12.5 °C) during the past decades, and population density of eels tended to decline during the 2000s [41]. However, the attributes of the habitat were changing during the past decades owing to the reduced nutrient loading to the lake [20, 21]. The changed trophic state of the lake induced a serious feeding stress regarding the eel population of Lake Balaton due to the drastic reduction in Chironomids, representing their important food resource [41]. Food deprivation can play a role in the formation of vaterite inclusions. On the one hand it could obviously cause decreased health status, on the other hand some eels could not intake sufficient amounts of essential amino acids and it might indirectly cause the co-existence of $CaCO_3$ polymorphs in otoliths.

At this stage it is difficult to make a clear decision which is the main determinant factor, or how these effects are combined. However, a potential bacterial infection in the eel's endolympathic organ surely deserves future consideration since eel populations have precipitously declined over the last couple of decades and the reasons are not clearly understood [10].

Although inclusions from otoliths of European eel bearing a fusiform shape have never been reported formally earlier, similar features can be clearly seen beside the much larger mosaic inclusions in SEM images of otolith section from European eels

(Fig. 2f in [50]) and to a lesser degree in light microscopic section (Fig. 2a in [40]; Fig. 5b in [27]) of specimens from the same species caught in the Baltic Sea. Moreover, strikingly similar objects have been documented in otolith sections of shortfin eel *(Anguilla australis),* Tarawera River, New Zealand [1]. It suggests that this new type of vaterite inclusion might be more widespread and not restricted to the eels from Lake Balaton.

Microchemical analyses of anguillid otolith transects have commonly been used to evaluate their residence and migratory history between habitats of different salinity [2, 23, 43]. However, as vaterite and aragonite have a different trace element substitution due to their distinct crystal lattice structure the new type of vateritic inclusions, obviously, also requires caution to avoid misidentification in the specimen's migration history, similarly to mosaics of vateritic inclusions [24, 50]. It means technically, that one should also pay attention to avoid fusiform inclusions and maintain the mandatory homogeneous mineralogy [38, 52] when designating laser ablation paths, for instance, to track trace element profiles.

The origin and physiological significance of this new morphological type of vateritic inclusions found in eel otoliths is still an open question. Their fusiform shape, porous structure, characteristic core and the vateritic mineralogy, however, recall the characteristics described from bacterially mediated biomineralized calcium carbonate spherulites [39]. Further studies are needed to verify whether similar inclusions are present in otoliths of other eel populations or other teleosts.

ACKNOWLEDGEMENTS

Pieter Gaemers is acknowledged for comments on an earlier version of the manuscript. The research has been supported by Mohamed bin Zayed Species Conservation Fund (project no. 162512761), Research Centre of Excellence (11476-3/2016/FEKUT), Foundation for the Development of Animal Sciences, and "Lendület" program (LP2012-27/2012) by the Hungarian Academy of Sciences. This is contribution No. 49. of 2ka Palæoclimatology Research Group.

REFERENCES

1. Achenbach, P. (2012) An analysis of otoliths from two eels (*Anguilla australis* and *Anguilla dieffenbachii*) recovered from a hydroelectric dam turbine in the Tarawera River, New Zealand. Available at http://frontiersabroad.com/wp-content/uploads/2012/09/ParisAchenbach.pdf
2. Arai, T., Kotake, A., McCarthy, T. K. (2006) Habitat use by the European eel *Anguilla anguilla* in Irish waters. *Estuar. Coast. Shelf. Sci. 67*, 569–578.
3. Baronnet, A., Cuif, J. P., Dauphin, Y., Farre, B., Nouet, J. (2008) Crystallization of biogenic Ca-carbonate within organo-mineral micro-domains. Structure of the calcite prisms of the Pelecypod Pinctada margaritifera (Mollusca) at the submicron to nanometre ranges. *Mineral. Mag. 72,* 617–626.
4. Bearez, P., Carlier, G., Lorand, J. P., Parodi, G. C. (2005) Destructive and non-destructive microanalysis of biocarbonates applied to anomalous otoliths of archaeological and modern sciaenids (Teleostei) from Peru and Chile. *C. R. Biol. 328*, 243–252.
5. Borelli, G., Mayer-Gostan, N., De Pontual, H., Boeuf, G., Payan, P. (2001) Biochemical relationships between endolymph and otolith matrix in the trout (*Oncorhynchus mykiss*) and turbot (*Psetta maxima*). *Calcif. Tissue Int. 69,* 356–364.

6. Burgess, K. M. N., Bryce, D. L. (2015) On the crystal structure of the vaterite polymorph of $CaCO_3$: A calcium-43 solid-state NMR and computational assessment. *Solid State Nucl. Magn. Reson. 65,* 75–83.
7. Campana, S. E. (1999) Chemistry and composition of fish otoliths: pathways, mechanisms and applications. *Mar. Ecol. Prog. Ser. 188*, 263–297.
8. Cartwright, J. H. E., Checa, A. G. (2007) The dynamics of nacre self-assembly. *J. R. Soc. Interface 4*, 491–504.
9. Dauphin, Y. (2008) The nanostructural unity of mollusc shells. *Mineral. Mag. 72*, 243–246.
10. Dekker, W. (2009) Worldwide decline of eel resources necessitates immediate action. Quebec Declaration of Concern. In: Casselman, J. M., Cairns, D. K. (eds) *Eels at the Edge; Science, Status, and Conservation Concerns*. American Fisheries Society, Bethesda, Maryland. pp. 447–448.
11. Durif, C. F., van Ginneken, V., Dufour, S., Müller, T., Elie, P. (2009) Seasonal evolution and individual differences in silvering eels from different locations. In: van den Thillart, G., Dufour, S., Rankin, J. C. (eds) *Spawning Migration of the European Eel.* Springer, Netherlands. pp. 13–38.
12. Falini, G., Fermani, S., Vanzo, S., Miletic, M., Zaffino, G. (2005) Influence on the formation of aragonite or vaterite by otolith macromolecules. *Eur. J. Inorg. Chem. 2005,* 162–167.
13. Gabrielli, C., Jaouhari, R., Joiret, S., Maurin, G. (2000) In situ Raman spectroscopy applied to electrochemical scaling. Determination of the structure of vaterite. *J. Raman Spectrosc. 31*, 497–501.
14. Gauldie, R. W. (1986) Vaterite otoliths from Chinook salmon (Oncorhynchus tshawytscha). *N. Z. J. Mar. Freshwater Res. 20*, 209–217.
15. Gauldie, R. W. (1993) Polymorphic crystalline-structure of fish otoliths. *J. Morphol. 218,* 1–28.
16. Gauldie, R. W., Dunlop, D., Tse, J. (1986) The simultaneous occurrence of otoconia and otoliths in four teleost fish species. *N. Z. J. Mar. Freshwater Res. 20,* 93–99.
17. Gauldie, R. W., Sharma, S. K., Volk, E. (1997) Micro-Raman spectral study of vaterite and aragonite otoliths of the coho salmon, Oncorhynchus kisutch. *Comp. Biochem. Physiol., Part A Physiol. 139118,* 753–757.
18. Gherdán, K. (2010) Archaeometry on the nanoscale: New possibility in Hungary in the research of cultural heritage materials: FIB/SEM (focused ion beam microscope/scanning electron microscope) dual beam instrument at Eötvös Loránd University. *Archeometriai Műhely 7,* 157–159.
19. Giralt, S., Julià, R., Klerkx, J. (2001) Microbial biscuits of vaterite in Lake Issyk-Kul (Republic of Kyrgyzstan). *J. Sediment Res. 71,* 430–435.
20. Hatvani, I. G., Clement, A., Kovács, J., Kovács, I. S., Korponai, J. (2014) Assessing water-quality data: the relationship between the water quality amelioration of Lake Balaton and the construction of its mitigation wetland. *J. Great Lakes Res. 40*, 115–125.
21. Hatvani, I. G., Kovács, J., Márkus, L., Clement, A., Hoffmann, R., Korponai, J. (2015) Assessing the relationship of background factors governing the water quality of an agricultural watershed with changes in catchment property (W-Hungary). *J. Hydrol. 521*, 460–469.
22. Havancsák, K., Baris, A., Kalácska, S. (2013) Dual beam scanning electonmicroscope at Eötvös Loránd University. *Archeometriai Műhely 10*, 95–102
23. Jessop, B. M., Cairns, D. K., Thibault, I., Tzeng, W. N. (2008) Life history of American eel Anguilla rostrata: new insights from otolith microchemistry. *Aquat. Biol. 1,* 205–216.
24. Jessop, B. M., Shiao, J. C., Iizuka, Y., Tzeng, W. N. (2008) Prevalence and intensity of occurrence of vaterite inclusions in aragonite otoliths of American eels Anguilla rostrata. *Aquat. Biol. 2,* 171–178
25. Kabalah-Amitai, L., Mayzel, B., Kauffmann, Y., Fitch, A. N., Bloch, L., Gilbert, P., Pokroy, B. (2013) Vaterite crystals contain two interspersed crystal structures. *Science 340,* 454–457.
26. Lenaz, D., Miletic, M., Pizzul, E., Vanzo, S., Adami, G. (2006) Mineralogy and geochemistry of otoliths in freshwater fish from Northern Italy. *Eur. J. Mineral. 18,* 143–148.
27. Lin, Y., Shiao, J., Plikshs, M., Minde, A., Iizuka, Y., Rashal, I., Tzeng, W. (2011) Otolith Sr:Ca ratios as natural mark to discriminate the restocked and naturally recruited European eels in Latvia. *Am. Fish. Soc. Symp. 76,* 1–14.

28. Lowenstein, O. (1971) The labyrinth. In: Hoar, W. S., Randall, D. J. (eds) *Fish Physiology, Vol. V. Sensory Systems and Electric Organs.* Academic Press, NY, pp. 207–240.
29. Ma, T., Kuroki, M., Miller, M. J., Ishida, R., Tsukamoto, K. (2008) Morphology and microchemistry of abnormal otoliths in the ayu, Plecoglossus altivelis. *Environ. Biol. Fish. 83,* 155–167.
30. Ma, Y., Berland, S., Andrieu, J.-P., Feng, Q., Bédouet, L. (2013) What is the difference in organic matrix of aragonite vs. vaterite polymorph in natural shell and pearl? Study of the pearl-forming freshwater bivalve mollusc Hyriopsis cumingii. *Mat. Sci. Eng. C-Mater. Biol. Appl. 33,* 1521–1529.
31. Melancon, S., Fryer, B. J., Gagnon, J. E., Ludsin, S. A. (2008) Mineralogical approaches to the study of biomineralization in fish otoliths. *Mineral. Mag. 72,* 627–637.
32. Motta, C. M., Avallone, B., Balassone, G., Balsamo, G., Fascio, U., Simoniello, P., Tammaro S., Marmo, F. (2009) Morphological and biochemical analyses of otoliths of the ice-fish Chionodraco hamatus confirm a common origin with red-blooded species. *J. Anatom. 214,* 153–162.
33. Mugiya, Y. (1972) On aberrant sagittas of teleostean fishes. *Japan. J. Ichthyol. 19,* 11–14.
34. Murayama, E., Takagi, Y., Ohira, T., Davis, J. G., Greene, M. I., Nagasawa, H. (2002) Fish otolith contains a unique structural protein, otolin-1. *Eur. J. Biochem. 269,* 688–696.
35. Parker, J., Pollard, J. W., Friesen, J. D., Stanners, C. P. (1978) Stuttering: high-level mistranslation in animal and bacterial cells. *Proc. Nat. Acad. Sci. 75,* 1091–1095.
36. Payan, P., De Pontual, H., Bœuf, G., Mayer-Gostan, N. (2004) Endolymph chemistry and otolith growth in fish. *C. R. Palevol. 3*, 535–547.
37. Pisam, M., Payan, P., LeMoal, C., Edeyer, A., Boeuf, G., Mayer-Gostan, N. (1998) Ultrastructural study of the saccular epithelium of the inner ear of two teleosts, Oncorhynchus mykiss and Psetta maxima. *Cell Tiss Res. 294,* 261–270.
38. Pracheil, B. M., Chakoumakos, B. C., Feygenson, M., Whitledge, G. W., Koenigs, R. P., Bruch, R. M. (2017) Sturgeon and paddlefish (Acipenseridae) sagittal otoliths are composed of the calcium carbonate polymorphs vaterite and calcite. *J. Fish Biol. 90,* 549–558. doi:10.1111/jfb.13085
39. Rodriguez-Navarro, C., Jimenez-Lopez, C., Rodriguez-Navarro, A., Gonzalez-Munoz, M. T., Rodriguez-Gallego, M. (2007) Bacterially mediated mineralization of vaterite. *Geochim. Cosmochim. Acta 71,* 1197–1213.
40. Shiao, J. C., Lozys, L., Iizuka, Y., Tzeng, W. N. (2006) Migratory patterns and contribution of stocking to the population of European eel in Lithuanian waters as indicated by otolith Sr : Ca ratios. *J. Fish Biol. 69,* 749–769.
41. Specziár, A. (2010) Fish fauna of Lake Balaton: stock composition, living conditions of fish and directives of the modern utilization of the fish stock. *Acta Biol. Debrecina Suppl. Oecologica Hungarica 23 (Hydrobiological Monographs vol. 2)*, 7–185.
42. Sweeting, R. M., Beamish, R. J., Neville, C. M. (2004) Crystalline otoliths in teleosts: Comparisons between hatchery and wild coho salmon (Oncorhynchus kisutch) in the Strait of Georgia. *Rev. Fish Biol. Fish. 14,* 361–369
43. Tabouret, H., Bareille, G., Claverie, F., Pecheyran, C., Prouzet, P., Donard, O. F. X. (2010) Simultaneous use of strontium:calcium and barium:calcium ratios in otoliths as markers of habitat: Application to the European eel (Anguilla anguilla) in the Adour basin, South West France. *Mar. Environ. Res. 70*, 35–45.
44. Takagi, Y. (2002) Otolith formation and endolymph chemistry: a strong correlation between the aragonite saturation state and pH in the endolymph of the trout otolith organ. *Mar. Ecol. Prog. Ser. 231*, 237–245.
45. Takagi, Y., Tohse, H., Murayama, E., Ohira, T., Nagasawa, H. (2005) Diel changes in endolymph aragonite saturation rate and mRNA expression of otolith matrix proteins in the trout otolith organ. *Mar. Ecol. Prog. Series 294*, 249–256.
46. Thalmann, R., Thalmann, I., Lu, W. (2011) Significance of tertiary conformation of otoconial matrix proteins – clinical implications. *Acta Oto-Laryngol. 131*, 382–390.
47. Tomas, J., Geffen, A. J. (2003) Morphometry and composition of aragonite and vaterite otoliths of deformed laboratory reared juvenile herring from two populations. *J. Fish Biol. 63,* 1383–1401.

48. Tomas, J., Geffen, A. J., Allen, I. S., Berges, J. (2004) Analysis of the soluble matrix of vaterite otoliths of juvenile herring (Clupea harengus): do crystalline otoliths have less protein? *Comp. Biochem. Physiol., Part A Mol. Integr. Physiol. 139,* 301–308.
49. Tong, H., Ma, W., Wang, L., Wan, P., Hu, J., Cao, L. (2004) Control over the crystal phase, shape, size and aggregation of calcium carbonate via a l-aspartic acid inducing process. *Biomaterials 25,* 3923–3929.
50. Tzeng, W. N., Chang, C. W., Wang, C. H., Shiao, J. C., Iizuka, Y., Yang, Y. J., You, C. F., Lozys, L. (2007) Misidentification of the migratory history of anguillid eels by Sr/Ca ratios of vaterite otoliths. *Mar. Ecol. Prog. Ser. 348,* 285–295.
51. Urmos, J., Sharma, S. K., Mackenzie, F. T. (1991) Characterization of some biogenic carbonates with raman-spectroscopy. *Am. Mineral. 76,* 641–646.
52. Veinott, G. I., Porter, T. R., Nasdala, L. (2009) Using Mg as a proxy for crystal structure and Sr as an indicator of marine growth in vaterite and aragonite otoliths of aquaculture rainbow trout. *Trans. Am. Fish. Soc. 138,* 1157–1165.